ELSEVIER

PII: S0032-3861(97)00430-8

Polymer Vol. 39 Nos. 6–7, pp. 1351–1355, 1998
© 1997 Elsevier Science Ltd
Printed in Great Britain. All rights reserved
0032-3861/97/$17.00+0.00

Application of a high-tension annealing method to nylon 66 fibres

Akihiro Suzuki*, Hideo Murata and Toshio Kunugi
Department of Applied Chemistry and Biotechnology, Faculty of Engineering, Yamanashi University, 4-3-11 Takeda, Kofu 400, Kofu, Japan
(Received 5 November 1996; revised 27 January 1997)

A high-tension annealing (HTA) method has been applied to nylon 66 fibres to improve their mechanical properties. The HTA was carried out three times under high tension close to the tensile strength at break. The nylon 66 fibre used for the HTA treatment was previously zone-drawn twice at 210°C under applied tensions of 14.5 MPa and 182.2 MPa. To orient amorphous chains selectively, two HTA treatments were carried out; the first HTA (HTA1) at 100°C under an applied tension of 143.3 MPa, and the second (HTA2) treatment at 110°C under 142.0 MPa. The third (HTA3) treatment was carried out at 190°C under 75.1 MPa to crystallize the amorphous regions oriented by the HTA1 and HTA2 treatments. The resulting HTA3 fibre had a draw ratio of 7.3, a value of birefringence of 0.0761, and a degree of crystallinity of 40.4%. The orientation factor of crystallites almost approached unity in the first high-temperature zone-drawing (HT-ZD1) stage, but that of amorphous regions (f_a) was 0.575 in the HT-ZD1 stage. The f_a increased with the processing and finally reached a high value of 0.852 for the HTA3 fibre. Dynamic moduli increased with the processing, and the dynamic modulus of the HTA3 fibre was 21.7 GPa at 25°C and 15.0 GPa even at 200°C. © 1997 Elsevier Science Ltd. All rights reserved.

(Keywords: high-temperature zone-drawing; high-tension annealing; nylon 66 fibre)

INTRODUCTION

Many techniques for the production of high-modulus nylon fibres have so far been proposed. Dry-spinning [1], zone-drawing and zone-annealing [2], spinning from nylon 6/lithium chloride or nylon 6/lithium bromide mixtures [3,4], solid-state coextrusion [5], and high-temperature zone-drawing [6] are some of the techniques leading to high-modulus and high-strength fibres. However, there is a very considerable gap between the achieved moduli and the theoretical moduli of nylon fibres [7].

The polymers with a degree of crystallinity of 70% and more form the intercrystalline bridges connecting longitudinally crystal regions [8]. Therefore, the moduli of polymers with high crystallinity can be expected to approach the theoretical values owing to the existence of the crystallite bridges in the polymers. Actually, it was recognized that high molecular weight it-polypropylene produced by ultra-drawing has a Young's modulus of 36 GPa[9], 87% of a theoretical value of 42 GPa [10]. However, since most polymers in common use such as nylon 6, nylon 66 and poly(ethylene terephthalate) have only the degrees of crystallinity of the order of 50–60%, their mechanical properties chiefly depend on the amorphous regions rather than crystalline regions. Therefore, the improvements of the mechanical properties would be achieved by increasing the number of the tie chains in the amorphous regions and making uniform those lengths so that applied stress may be loaded equally on the fibre.

To produce the high-modulus fibres, we proposed a high-tension annealing (HTA) method. The HTA treatments are characterized by the treatment of fibres under extremely high tension close to the strength at break. The object is to extend fully the tie chains in the amorphous regions. Using the HTA treatment, the amorphous chains which have been difficult to extend by the zone-drawing and zone-annealing methods can be arranged highly along the fibre axis. The HTA treatment has already been applied to crystalline polymers such as poly(ethylene terephthalate) [11], poly(vinyl alcohol) [12], and nylon 6 [13], and their amorphous orientation factors were found to reach high values, and then high-modulus fibres were obtained.

The purpose of this paper is to produce high-modulus nylon 66 fibres by using the HTA method. The change in the microstructure with the processing was also studied using d.s.c. and X-ray diffraction measurements.

EXPERIMENTAL

Material

The original material used in the present study is as-spun nylon 66 single fibre supplied by Toray Ltd. The original fibre has a diameter of about 0.327 mm, crystallinity of 27%, and birefringence of 0.0012. The original fibre was found to be isotropic from a wide angle X-ray diffraction photograph.

High-temperature zone-drawing and high-tension annealing treatments

The original fibres were treated twice with high-temperature zone-drawing (HT-ZD) before HTA treatments. The HT-ZD treatment was described previously[14,15]. The HT-ZD treatments were carried out by moving the zone heater at a speed of 25 mm min^{-1} along the drawing direction. A schematic diagram of the experimental apparatus used for the HTA treatments is shown in *Figure 1*. It consists of a load cell connected to a recorder,

* To whom correspondence should be addressed

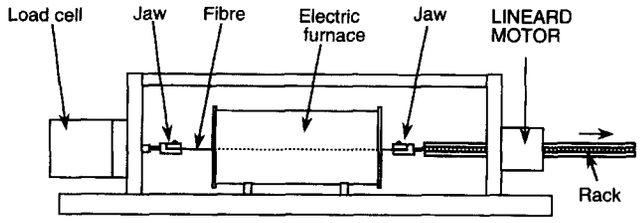

Figure 1 Apparatus used for the high-tension annealing

an electric furnace 20 mm long, and a Lineard Motor (Oriental Motor Co. Ltd) which consists of a rack-and-pinion unit and a speed controller. The rack-and-pinion unit converts rotational motion of the motor into linear motion. One end of a single fibre was fixed at the jaw equipped with the load cell, and the other at the jaw equipped with the edge of the rack, and the fibre was drawn at a constant speed. When the temperature of the electric furnace reached the desired treating temperature, the fibre was drawn at a drawing speed of 10 mm min^{-1}. When the tension applied to the fibre reached a desired value which is in the range of 75–95% of the strength at break (σ_b), the stretching was stopped, and then the fibre was kept under constant length for a given time. This desired value is called an initial applied tension and designated as σ_0.

Measurements

The draw ratio was determined in the usual way by measuring the displacement of ink marks placed 10 mm apart on the specimens prior to drawing. The birefringence was measured with a usual polarizing microscope equipped with a Berek compensator. The density was measured at 25°C by a flotation method using an n-heptane and carbon tetrachloride mixture. The crystallinity in weight fraction (X_w) was calculated from the density (d) using the following equation with a crystal density (d_c) of 1.24 g cm^{-3} and an amorphous density (d_a) of 1.09 g cm^{-3} [16].

$$X_w = \frac{d_c(d-d_a)}{d(d_c-d_a)} \times 100 \quad (1)$$

Thermal shrinkage was measured with a Rigaku SS-TMA at a heating rate of 5°C min^{-1}. The samples with a 15 mm gauge length between two jaws were held under a tension of 5 g cm^{-2}, which was the minimum tension to stretch a fibre tightly.

The apparent crystallite sizes were estimated from the broadening of the diffraction peaks by applying Scherrer's equation:

$$D_{hkl} = 0.9\lambda/(\beta \cos \theta_{hkl}) \quad (2)$$

where D_{hkl} is the crystallite width normal to the (hkl) plane, λ is the X-ray wavelength (1.542 Å), θ_{hkl} is the Bragg angle of the (hkl) plane, and β is the observed half-width of the peak, which was corrected for the instrumental broadening.

The orientation factors of crystallites (f_c) were evaluated by using the Wilchinsky method [17] from wide angle X-ray diffraction patterns. The orientation factors of amorphous chains (f_a) were determined according to the following equation:

$$f_a = \frac{\Delta n - \Delta n_c^o f_c X_v}{\Delta n_a^o (1 - X_v)} \quad (3)$$

where Δn is the optical birefringence, X_v is the crystallinity in volume fraction, f_c is the orientation factor of crystallites, and Δn_c^o and Δn_a^o are the intrinsic optical birefringences of the crystalline and amorphous regions, respectively. The values of f_a were determined using $\Delta n_c^o = 0.096$ and $\Delta n_a^o = 0.077$ [18].

The tensile properties were determined with a Tensilon tensile testing machine. Young's modulus, tensile strength and elongation at break were calculated from the stress–strain curves obtained at 23°C, r.h. 65%. The dynamic viscoelastic properties were measured at 110 Hz with a dynamic viscoelastometer VIBRON DDV-II (Orientec Co. Ltd.). Measurements were carried out over a temperature range of 25°C to about 250°C at intervals of 5°C, and the average heating rate was 2°C min^{-1}. A single fibre was held in a 20 mm gauge length between the jaws.

RESULTS AND DISCUSSION

Conditions for the high-temperature zone-drawing and high-tension annealing

The optimum conditions for the HT-ZD treatments were the same as those determined in the previous paper [15], which are given in *Table 1*. The HTA treatments were carried out three times; the first (HTA1) and second (HTA2) treatments were carried out at temperatures close to the glass transition temperature (T_g) to orient the amorphous chains further without fracture of the crystal regions. The third (HTA3) treatment was performed at an elevated temperature to crystallize the amorphous chains which were highly oriented by the HTA1 and HTA2 treatments. The optimum condition for each step was determined by measuring the birefringence of the fibres treated under various conditions. The condition giving the highest birefringence was chosen as an optimum one for the each treatment. *Figure 2* shows the changes in the birefringence of the fibres treated at various temperatures (T_{HTA}) ranging from 80 to 120°C with the initial applied tension (σ_0) in the HTA1 treatment. The σ_0s are in the range of 75–95% of the strength at break (σ_b).

Table 1 Optimum conditions for high-temperature zone-drawing

	Drawing temperature (°C)	Applied tension (MPa)	Heater speed (mm min^{-1})
HT-ZD1	210	14.5	25
HT-ZD2	210	182.2	25

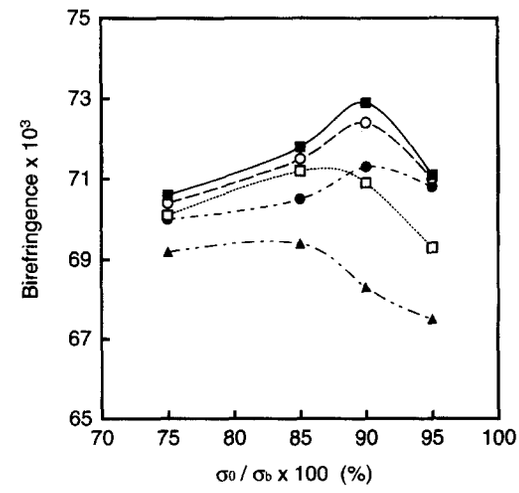

Figure 2 Changes in the birefringence with σ_0/σ_b for the fibres obtained at various drawing temperatures in the HTA1 treatment: ●, 80°C; ○, 90°C; ■, 100°C; □, 110°C; ▲, 120°C

The σ_b value for the HTA1 treatment at a given temperature was equal to that of the HT-ZD2 fibre measured at the same temperature. The birefringence of each fibre when treated at 80, 90 and 100°C shows a maximum value at $\sigma_0 = 0.9\sigma_b$; the fibre of $T_{HTA} = 100$°C at $\sigma_0 = 0.9\sigma_b$ (= 143.3 MPa) gives the highest birefringence of 0.073. *Figure 3* shows the change in applied tension (σ) with time during the HTA1 treatment at 100°C. The σ decreased rapidly at first (within 2 min) and reached a pseudo equilibrium value (σ_e) in about 30 min. The decrease in σ indicates that the molecular chains were further elongated without orientation relaxation because the birefringence of the HT-ZD2 fibre increased by the HTA1 treatment, as will be described below. The optimum treating time for the HTA1 treatment was determined as 30 min. Further, the optimum conditions of the HTA2 and HTA3 treatments were also determined in the same way as in the case of the HTA1, and are summarized in *Table 2*.

Microstructure for the HT-ZD and HTA fibres

Figure 4 shows the relation between the draw ratio and birefringence of the HT-ZD and HTA fibres. The birefringence increases with increasing draw ratio; it increases

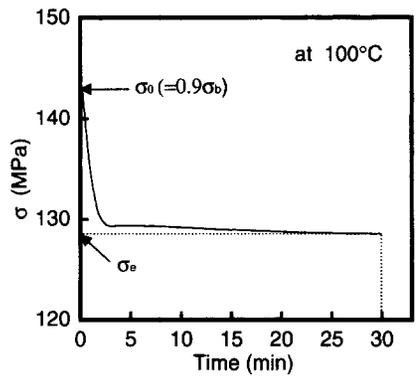

Figure 3 Change in stress with treating time during the HTA1 treatment

Table 2 Optimum conditions for HTA treatments

	Treating temperature (°C)	Initial applied tension, σ_0 (MPa)	Treating time (min)
HTA1	100	143.3 (= $0.9\sigma_b$)	30
HTA2	110	142.0 (= $0.9\sigma_b$)	30
HTA3	190	75.1 (= $0.9\sigma_b$)	10

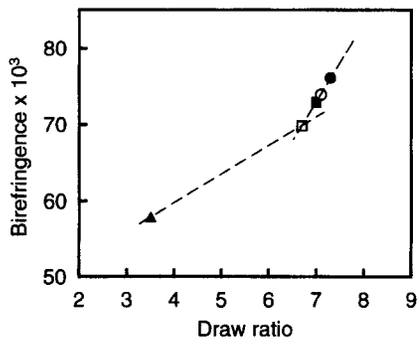

Figure 4 Relation between draw ratio and birefringence for the original, HT-ZD and HTA fibres: ▲, HT-ZD1; □, HT-ZD2; ■, HTA1; ○, HTA2; ●, HTA3

especially more rapidly above a draw ratio of 7. In general, the birefringence increases gradually with increasing draw ratio at low draw ratios, but it levels off to reach a saturated value at higher ratios [19]. In this experiment, however, the results are opposite; the slope of the birefringence *versus* draw ratio curve for higher draw ratios is larger than that for lower draw ratios. Such excess increment of birefringence implies that the HTA treatments were effective in drawing chain molecules without the relaxation of orientation.

The degrees of crystallinity, crystallite sizes normal to the (100) and the (010/110) planes (D_{100} and $D_{010/110}$), and orientation factors of crystallites and amorphous regions for the HT-ZD and HTA treated fibres are summarized in *Table 3*. The degrees of crystallinity and crystallite sizes increase stepwise with the processing. These values in the HTA1 and HTA2 treatments increase slightly compared with the HT-ZD and HTA-3 treatments. Finally, the degree of crystallinity reaches 40.4% for the HTA3 fibre. The change in crystallinity with the processing suggests that the amorphous chains which had been highly oriented by the HTA1 and HTA2 treatments were crystallized additionally during the HTA3 treatment. Although the birefringence increased from 0.69 for the HT-ZD2 fibre to 0.74 for the HTA2 fibre, no additional crystallization occurred. The increase in birefringence originates in the improvement of orientation of amorphous chains during the HTA1 and HTA2 treatments because the crystalline orientation factor already reaches the highest value, as described below.

The orientation factor of crystallites increases remarkably up to 0.971 with only the HT-ZD1 treatment and maintains its value even after the subsequent treatments; the

Table 3 Crystallinity, crystallite size of (100) and (010/110) planes orientation factors of crystallites and amorphous regions (f_c and f_a) of the original, HT-ZD, and HTA fibres

Fibre	Crystallinity (%)	Crystallite size (Å)		f_c	f_a
		D_{100}	$D_{010/110}$		
Original	26.8	—	—	—	
HT-ZD1	30.7	36.7	31.2	0.971	0.575
HT-ZD2	35.6	38.4	32.4	0.978	0.755
HTA1	36.3	42.5	32.4	0.976	0.812
HTA2	37.0	44.9	33.8	0.977	0.827
HTA3	40.4	47.5	40.5	0.976	0.852

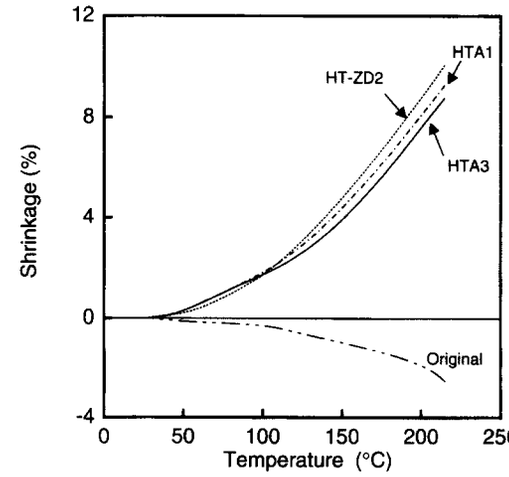

Figure 5 Temperature dependence of shrinkage for the original, HT-ZD and HTA fibres

crystallites are easily aligned in the drawing direction in the same manner as in the case of the HT-ZD nylon 66 fibres previously reported [15]. On the other hand, the amorphous orientation factor increases from 0.575 for the HT-ZD1 fibre to 0.852 for the HTA3 fibre strongly dependent on the processing.

Figure 5 shows the temperature dependence of the thermal shrinkage for the original, HT-ZD and HTA fibres. The original fibre extends gradually with increasing temperature and up to an extension of 2.5% at 215°C. On the other hand, the HT-ZD and HTA fibres shrink with temperature, and the thermal shrinkage is associated with chain folding in the amorphous regions [20]. The degree of shrinkage tends to decrease with the processing, and the HTA3 fibre with the highest crystallinity has the lowest shrinkage ratio of 8.8% at 215°C in comparison with other fibres. The thermal shrinkage closely depends on the degree of crystallinity and was prevented by the crystallites formed during the treatments [21]. A slight increase in the slope of the thermal shrinkage *versus* temperature curves for the treated fibres shows above 100°C. The slight increase is attributable to the rupture of hydrogen bonds inhibiting the chain refolding.

Mechanical properties for the HT-ZD and HTA fibres

The tensile properties of the HT-ZD and HTA fibres obtained are summarized in *Table 4*. Young's modulus and tensile strength increase with the processing. Young's modulus of the HTA3 fibre reaches 12.3 GPa and is higher than the value of 3.9 GPa for the commercial grade fibre [22]. However, there is a very considerable gap between the modulus of the HTA3 fibre and the theoretical value (= 172 GPa) of the nylon 66 [23].

Figure 6 shows the temperature dependence of storage modulus (E'), for the original, HT-ZD, and HTA fibres. The E' values over a wide temperature range increase progressively with the processing. Finally, the E' value of the HTA3 fibre reaches 21.7 GPa at 25°C and holds 15 GPa even at 200°C. The E' values of all the fibres, except the HTA2 fibre, decrease gradually with increasing temperature. However, that for the HTA2 fibre falls markedly in the α relaxation region, approaching that of HTA1 fibre at elevated temperatures. On the other hand, the E' of the HTA3 fibre decreases almost linearly with temperature without a marked fall in the α relaxation region. *Figure 7* shows the temperature dependence of tan δ for the original, HT-ZD, and HTA fibres. These fibres show α peaks in the temperature range of 80–120°C, which is considered to originate from a rupture of interchain hydrogen bonding due to the increase of motions of chain segments in amorphous regions [24]. The α peak shifts to a higher temperature, with decreasing its peak height progressively, and becomes much broader with the processing. The α peak of the HTA3 fibre occurs at 120°C and is the lowest in the peak height. The changes in position and in profile of the α peak with the processing designate that the molecular mobility in the amorphous regions is restricted by the surrounding crystallites.

CONCLUSION

The HTA method has been applied to nylon 66 fibres to improve their mechanical properties, and the results are as follows.

(1) The degree of crystallinity increased from 27% to 36% by two HT-ZD treatments, and finally up to 40% by the HTA3 treatment, though it hardly changed by the HTA1 and HTA2 treatments.
(2) The orientation factor of crystallites rose remarkably up to 0.971 by only the HT-ZD1 treatment, while that of amorphous regions increased progressively with the processing and reached 0.852 in the HTA3 fibre.
(3) The storage modulus of the HTA3 fibre reached 21.7 GPa at 25°C and held 15 GPa even at 200°C.

Table 4 Mechanical properties of the original, HT-ZD and HTA fibres

Fibre	Young's modulus (GPa)	Tensile strength (GPa)	Elongation at break (%)
Original	1.1	0.18	385.6
HT-ZD1	4.7	0.54	34.5
HT-ZD2	6.4	0.75	12.9
HTA1	8.2	1.10	13.4
HTA2	9.5	1.18	12.6
HTA3	12.3	1.42	13.1

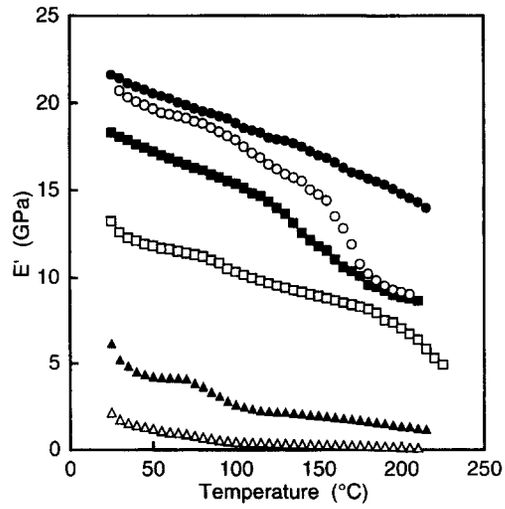

Figure 6 Temperature dependence of storage modulus (E') for the original, HT-ZD and HTA fibres: △, original; ▲, HT-ZD1; □, HT-ZD2; ■, HTA1; ○, HTA2; ●, HTA3

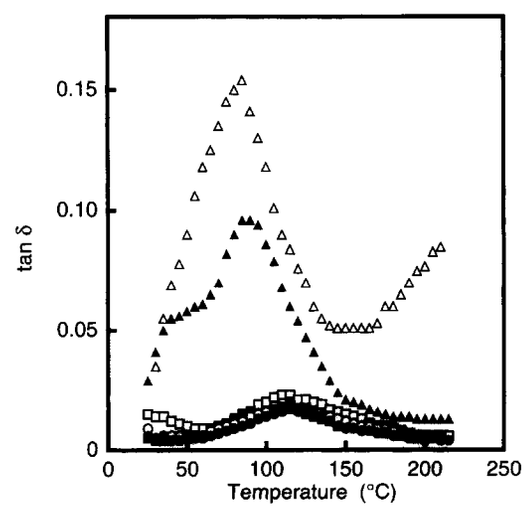

Figure 7 Temperature dependence of loss tangent (tan δ) for the original, HT-ZD and HTA fibres: △, original; ▲, HT-ZD1; □, HT-ZD2; ■, HTA1; ○, HTA2; ●, HTA3

The α peak in the tan δ–temperature curve shifted to a higher temperature, reducing its magnitude\Psi progressively with the processing. The HTA method was found to be effective in the improvement of nylon 66 fibres.

ACKNOWLEDGEMENTS

We are grateful to Toray Ltd. for supplying nylon 66 fibres to us.

REFERENCES

1. Gogolewski, S. and Penneings, A. J., *Polymer*, 1985, **26**, 1394.
2. Kunugi, T., Akiyama, I. and Hashimoto, M., *Polymer*, 1982, **23**, 1193.
3. Richardson, A. and Ward, I. M., *J. Polym. Sci.*, 1981, **19**, 1549.
4. Acierno, D., La Mantia, F. P., Polizotti, G., Alfonso, G. C. and Ciferre, A., *J. Polym. Sci. Polym. Lett. Ed.*, 1977, **15**, 323.
5. Zachariades, A. E. and Poter, R. S., *J. Appl. Polym. Sci.*, 1979, **24**, 1371.
6. Kunugi, T., Akiyama, I. and Hashimoto, M., *Polymer*, 1982, **23**, 1193.
7. Kaji, K. and Sakurada, I., *Makromol. Chem.*, 1978, **179**, 209.
8. Gibson, A. G., Davies, G. R. and Ward, I. M., *Polymer*, 1978, **19**, 683.
9. Peguy, A. and John Manley, R., *Polym. Communications*, 1984, **25**, 39.
10. Sakurada, I., Ito, T. and Nakamae, K., *J. Polym. Sci. Part C*, 1966, **15**, 75.
11. Kunugi, T., Suzuki, A. and Tsuiki, T., *Kobunshi Ronbunsyu*, 1991, **48**, 703.
12. Suzuki, A., Kawasaki, S. and Kunugi, T., *Kobunshi Ronbunsyu*, 1994, **51**, 201.
13. Suzuki, A., Kondo, M. and Kunugi, T., *Kobunshi Ronbunsyu*, 1993, **50**, 93.
14. Suzuki, A. and Endo, A., *Polymer*, 1997, **38**, 3085.
15. Suzuki, A., Maruyama, S. and Kunugi, T., *Kobunshi Ronbunsyu*, 1992, **49**, 741.
16. Keller, A., *Growth and Perfection of Crystals*, ed. D. Turnbull. John Wiley, New York, 1958.
17. Wilchainsky, Z. W., *J. Appl. Phys.*, 1959, **30**, 79.
18. Matumoto, K., *Sen-i Gakkaishi*, 1970, **32**, T–365.
19. O'Neill, M. A., Duckett, R. A. and Ward, I. M., *Polymer*, 1988, **29**, 54.
20. Wilson, M. P. W., *Polymer*, 1974, **15**, 277.
21. Peszkin, P. N. and Schultz, J. M., *J. Polym. Sci. Part B*, 1986, **24**, 2591.
22. Mochizuki, M. and Kudo, K., *Sen-i Gakkaishi*, 1991, **47**, P–336.
23. Sakurada, I. and Kaji, K., *J. Polym. Sci. Part C*, 1970, **31**, 57.
24. Woodward, A. E. and Sauer, J. A., *J. Colloid. Sci.*, 1957, **12**, 363.